Earth Syst. Dynam. Discuss., 4, 717–742, 2013
www.earth-syst-dynam-discuss.net/4/717/2013/
doi:10.5194/esdd-4-717-2013

Earth System Dynamics Discussions
Open Access

Quantifying the "Energy-Return-on-Investment" of desert greening in the Sahara/Sahel using a Global Climate Model

S. P. K. Bowring[1], L. M. Miller[2], L. Ganzeveld[1], and A. Kleidon[2]

[1]Earth Systems Science Group, Wageningen University and Research Centre, Wageningen, the Netherlands
[2]Max Planck Institute for Biogeochemistry, Jena, Germany

Received: 30 July 2013 – Accepted: 31 July 2013 – Published: 8 August 2013

Correspondence to: S. P. K. Bowring (simon.bowring@wur.nl)

Published by Copernicus Publications on behalf of the European Geosciences Union.

Abstract

"Greening" the world's deserts has been proposed as a way to produce additional food, sequester carbon, and alter the climate of desert regions. Here, we quantify the potential benefits in terms of energetic quantities and compare these to the energetic costs. We then compare these using the metric of Energy-Return-On-Investment (EROI). We apply EROI to a series of global climate model simulations where the arid Sahara/Sahel region is irrigated with various rates of desalinated water to produce biomass. The energy content of this biomass is greater than the energy input rate for a minimum irrigation rate of about 200 mm yr^{-1} in the winter and 500 mm yr^{-1} in the summer, thereby yielding an EROI ratio > 1 : 1, expressing energetic sustainability. Quantified annually, the EROI was > 1 : 1 for irrigation rates more than 500 mm yr^{-1}, progressively increasing to a maximum of 1.8 : 1 with 900 mm yr^{-1}, and then decreasing with further increases in the irrigation rate. Including the precipitation feedback arising from changes in moisture-recycling within the study region approximately doubles these EROI ratios. This overall result varies spatially and temporally, so while the entire Sahara/Sahel region is irrigated equally, the western coastal region from June to August had the highest EROI. Other factors would complicate such a large-scale modification of the Earth System, but this sensitivity study concludes that with a required energy input, desert greening may be energetically sustainable. Furthermore, we suggest that this type of EROI-analysis could be applied as a metric to assess a diverse range of human alterations to, and interventions within, the Earth System.

1 Introduction

A general understanding that mankind is approaching or exceeding the carrying capacity of the Earth's various natural systems has motivated considerable investigation in the direction of "sustainable" processes at the conjunction of the human and earth systems. Many environmental problems involve energy, either explicitly (as in the combus-

ESDD
4, 717–742, 2013

tion of fossil fuels) or implicitly (in the inefficiency or "waste" in their usage). These are "direct" energy quantifications, insofar as we regard oil or electricity as "energy". However, other phenomena or materials can also be described in these energetic terms: it takes energy to evaporate water as steam, for example, while the condensation of that steam releases the same amount of energy. Biomass can be represented in a similar way because organisms store up energy in life and release it to the environment. Thus, although sustainability is guided by notions of increased process-efficiency, the use of energy as a common denominator for the terms of that efficiency allows one to directly quantify the sustainability of diverse processes, and their direct and indirect products. In addition, energy-denominated quantification implies the potential for commensurability and comparability between these processes. The goal of this paper is to quantify this energetic sustainability for one such process.

1.1 Energy-Return-On-Investment

The "return-on-investment" is commonly applied in economics, both for its historical and future relevance. A similar energetic quantification can also be applied to our actions and their results within the Earth System. This was first done by Hall et al. (1986) and is now known as Energy-Return-On-Investment, or EROI (Murphy and Hall, 2010). EROI quantifies the ratio between the actual and expected energetic outputs from a given action (E_{out}) and the actual and expected energetic inputs to that process (E_{in}), implying its sustainability in these terms if that value exceeds 1.0 (Murphy and Hall, 2010). It is defined in its simplest form as:

$$\mathrm{EROI} = \frac{E_{out}}{E_{in}}. \quad (1)$$

EROI is neither a complex nor particularly new concept, although actually applying it empirically to a scenario can be difficult (see Discussion). When applied to a given mechanism or process, EROI provides an aggregated thermodynamic metric that can

ESDD
4, 717–742, 2013

compare widely varying techno-economic processes in their interaction with the environment (e.g. Bakshi et al., 2011). Variations in the definition of the E_{in} and E_{out} in Eq. (1) include *energy* (Murphy and Hall, 2010), *exergy* (Gutowski et al., 2009) and *emergy* (Odum, 1996). EROI or slight variations in it have been predominantly used as tools for life-cycle analysis in process engineering, industrial ecology, and ecological economics (e.g. Valero and Valero, 2011; Patzek, 2008; Gutowski et al., 2009; Baum et al., 2009). EROI quantification can also be used in Earth System studies, from looking at the energy return on extracting natural stocks (e.g. oil) and flows (e.g. wind), to the embedding of such processes in specific space-time (e.g. geographical) contexts. We briefly expand on these examples with the following illustrations.

Applied to the context of oil and gas, its EROI in 1930 was $> 100:1$, showing that a very large energy output resulted from a small energy input. The increasing extraction and use of oil and gas made continual discoveries and extractions more difficult, so by 1970, the EROI had decreased to $30:1$. By 2005, the EROI for oil and gas had decreased further to between $18:1$ and $11:1$, as noted in Murphy and Hall (2010).

As a differing example, early wind turbines were relatively small in both height and blade length, resulting in an EROI of less than $10:1$. Engineering and technological advancements in wind turbine technology resulted in taller towers with longer blades, making the present-day EROI for wind turbines $\approx 20:1$ (Kubiszewski et al., 2010). Note that while technological and economies-of-scale type considerations could further increase the EROI, it cannot infinitely increase. The generation rate of wind power in the Earth System is limited (Peixoto and Oort, 1992), limiting the electricity production rate of wind turbines (Miller et al., 2011), which thereby limits the EROI regardless of the extraction technology utilized. This highlights the connection of EROI with the natural environment and the ability of a human-applied change to alter the EROI, making it a dynamic rather than static reflection of these considerations.

Still, both of the previous EROI examples are calculated globally and do not incorporate the spatial or temporal differences that are specific to each study region. For both the "oil and gas" and the "wind turbine" examples, the EROI may not be spatially or

ESDD
4, 717–742, 2013

temporally constant. That is, the "process" EROI (of the abstracted technological process) may not equal the "actual" EROI (the energetic input and output of that process in a specific space-time or contextual setting). We can clarify this last point with a final theoretical example.

Consider the EROI of a 100 km^2 photovoltaic array. The [manufacturing] energy input (E_{in}) would be relatively independent of the geographic location where the array is deployed. By contrast, the energy output (E_{out}), which should include the electricity production rate and land–atmosphere effects related to the alterations to the surface, could be quite geographically dependent. Deploying the photovoltaic array to Greenland would produce less electricity both seasonally and annually than the same array deployed in Mexico. Additionally, drastic differences in the land–atmosphere interactions would be expected. Quantifying how EROI varies both spatially and temporally between such large-scale human projects, while also including the differences in Earth System dynamics is of specific interest to us here.

Note that although commonly described as an efficiency indicator, we use the term "sustainability" for EROI, since this captures its ability to describe whether the energy input to a process can be sustained by its energy output, whereas an efficient process is not necessarily energetically sustainable in this context.

1.2 Desert greening

An increasing scarcity of energy sources globally, as well as the indirect consequences of combusting conventional sources, have motivated the exploration of means by which to optimally make use of the available incident solar radiation on Earth. On this trajectory, the increased utilization of sunlight influencing the deserts has obvious practical appeal, since they combine low biological productivity with high energy input. One scheme put forward as a means to make use of this is the irrigation of deserts to induce local plant productivity.

The term "Desert Greening" as we will use it here, refers to irrigating an arid region to grow biomass for food or biofuel, sequester carbon, and/or alter the land–atmosphere

ESDD
4, 717–742, 2013

interactions of the region. This has been investigated along a variety of theoretical and practical lines (e.g. Kleidon et al., 2000; Ornstein et al., 2009; Becker et al., 2012). Given the water-limitation of deserts, a common-sense source for irrigation is the desalination of seawater and its subsequent pumping to plant root zones. Thus, there are energy inputs required by desalination and pumping. Desert greening's output, in the form of plant material, can be described by the total energy latent in photosynthetic carbohydrate biomass, which in the same way as petroleum, can be converted into another form of energy via some process (e.g. the total energy that can be released by its combustion). An additional energy output in this particular scenario is that of precipitation feedbacks (described below) induced by water and energy balance changes; its energy value is simply a multiple of the input energy value.

Despite these straightforward observations regarding its energy inputs and outputs, the practicalities of actually implementing desert greening is currently disconnected from an EROI focus, which would ask: *Does the energy we put into this process actually exceed the energy we get out of it?* That is, is it energetically sustainable? To be clear, this does not ask if desert greening is sustainable by "natural" processes, but whether maintaining a green desert by technological intervention is energetically sustainable. As mentioned, desert greening could be seen as a means of providing food, fuel and carbon sequestration in regions where biological productivity is currently very low, and socio-economic activity extremely sparse. In the context of climatic change, food scarcity and rising populations, these possibilities imply that the desert greening concept is of considerable research interest in its own right.

The Methods section will describe the model and the associated experimental setup. In Results, we will show the EROI and climatic differences that result from increased rates of irrigation on the Sahara/Sahel study region. The Discussion puts these results into the context of previous biogeochemical and meteorological studies, including the limitations we perceive in interpreting our results. This study will then end with a brief Conclusion.

ESDD
4, 717–742, 2013

2 Methods

This paper explores the spatial and temporal variation of EROI to differential input rates of irrigation water. The energy values used in EROI-calculation were taken from the literature. Energy required per unit volume of desalinated and pumped water (E_{DS}) was taken from Ornstein et al. (2009) because their estimation included the energy required for pumping and pressurizing in the desalination process and for distribution to the mean height of the Saharan region (450 m), assuming use of current state-of-the-art technology (but not higher-efficiency drip irrigation). Thus $E_{DS} = 14.54\,\mathrm{MJ\,m^{-3}}$. The latent output energy of net plant productivity (E_{NPP}) was taken from Gebel and Yüce (2008) and further studied in Becker et al. (2012), because this was taken to be representative of Jatropha, which is an arid region plant. Thus $E_{NPP} = 18.5\,\mathrm{MJ\,kg^{-1}}$ The ratio of net primary productivity (NPP) output difference in each simulation ($\Delta\mathrm{NPP}_{sim}$) and the corresponding irrigation rate (IR_{sim}) can be inserted into Eq. (1) to give EROI_A:

$$\mathrm{EROI}_A = \frac{(\Delta\mathrm{NPP}_{sim} \cdot E_{NPP})}{(\mathrm{IR}_{sim} \cdot E_{DS})}. \quad (2)$$

We define a second EROI value, here designated as EROI_B, which adds the precipitation difference over the irrigated region to the NPP-output energy. An increase in precipitation ($P_{rec.}$) can be considered an energetic gain that increases at the same rate as the energetic cost of desalinating the seawater. If we consider the irrigated region as a closed system, and (as here) ignore capital and other energetic costs of the desalination process, this value is equivalent to the "exergy return on investment" discussed in Bakshi et al. (2011). The equation for EROI_B is given by:

$$\mathrm{EROI}_B = \frac{(\Delta\mathrm{NPP}_{sim} \cdot E_{NPP}) + (\Delta P_{rec.} \cdot E_{DS})}{(\mathrm{IR}_{sim} \cdot E_{DS})}. \quad (3)$$

Note therefore that the *rate-of-return* on the energy investment (as a percentage) is given by $(\mathrm{EROI}_{value} - 1) \cdot 100$.

ESDD
4, 717–742, 2013

Given the extreme nature of this experiment and the number of necessary simulations, we use the PlasSim global climate model of intermediate complexity (Lunkeit et al., 2007). This model is based on a low resolution general circulation model, a mixed-layer ocean with prescribed ocean heat transport, interactive sea-ice model, a simple land surface and vegetation model, and prescribed ice sheets. Simulations were completed using the T42 spectral resolution (2.8° longitude by 2.8° latitude) and ten atmospheric levels. To simulate irrigation, a constant in-flux of water to the soil moisture box was introduced. This increase in irrigation is limited to the region of the Sahara and Sahel, hereafter referred to as the *irrigated region*. The extent of the irrigated region is based on a global biome map taken from Zeng et al. (2008), as their focus was on modeling vegetation in arid regions.

Twenty model runs were completed for 50 simulation years, with the last 30 yr used for analysis to exclude model spin-up. The irrigation rate intervals were determined from expected feasible and necessary water inputs found in previous studies (primarily Ornstein et al., 2009; Becker et al., 2012) and from the output in our trial runs. These were set at 100 mm yr^{-1} intervals from 0–1500 mm yr^{-1}, and at 500 mm intervals from 1500–3500 mm yr^{-1}. The latter was done to reduce total runtime. All other model parameters were set at their default values. All of these simulations were compared to an additional control simulation without any irrigation.

3 Results

3.1 Regional sensitivities of EROI, temperature and energy balance

Figure 1a shows the sensitivity of $EROI_A$ and $EROI_B$ during Northern Hemisphere winter (DJF) and summer (JJA) to the input irrigation rate. $EROI_A$ (based on biomass energy) and $EROI_B$ (which includes the precipitation feedback) are both almost half as large during the Northern Hemisphere winter than the summer. Winter EROI is maximized at 700 mm yr^{-1} of irrigation, while summer EROI is maximized at 1000 mm yr^{-1}.

ESDD
4, 717–742, 2013

This applies to both $EROI_A$ and $EROI_B$. The annual mean optimal irrigation input for the maximum $EROI_{A,B}$ is 900 mm yr^{-1}. At irrigation rates (IR_{sim}) lower than 400 mm yr^{-1}, EROI is lower in the summer than that in winter. The cause for this is straightforward. As shown in Fig. 1a, for $IR_{sim} > 400$ mm yr^{-1} the precipitation enhancement is greater in the summer (JJA) than during the winter (DJF), and in Fig. 1b, at $IR_{sim} > 500$ mm yr^{-1} the summer NPP difference is also greater in the summer than that during winter.

What emerges from Fig. 1a is that optimal winter and summer irrigation input are different. The amount of water and consequently energy input actually needed, vary seasonally, with implications for optimal water use efficiency. In the Northern Hemisphere winter, the maximum $EROI_A$ is 1.3 : 1 and the maximum $EROI_B$ is 1.6 : 1. In the summer, the maximum $EROI_A$ is 1.8 : 1 and the maximum $EROI_B$ is 2.6 : 1. Quantified annually, EROI declines at irrigation rates above 900 mm yr^{-1}, but the rate of decline in EROI is flatter for the low compared to high irrigation rates, implying that more water is more energetically sustainable than less water, for values of irrigation input less than 500 mm yr^{-1}, and greater than 900 mm yr^{-1}. This is particularly evident during the summer.

Figure 2 shows the area-averaged seasonal precipitation difference, the latent and sensible heat fluxes, and surface temperature difference respectively. Declines in surface sensible heat are mirrored by increases in latent heat flux with increasing irrigation, which in turn depresses the surface temperature of the irrigated area. Changes in latent and sensible heat fluxes and surface temperature all saturate at between 1500–2000 mm yr^{-1}, which implies that evaporation is occuring at potential evapotranspiration, as well as a maximum in the cooling effect of water on the land surface at these irrigation rates. From Fig. 2d, we observe that surface temperature declines most during summer, reaching a maximum difference of about −10 K at an irrigation rate greater than 1400 mm yr^{-1}, whereas during winter this figure is about −7 K. This is expected, given the increased solar energy input during the Northern Hemisphere summer.

ESDD
4, 717–742, 2013

3.2 Spatio-temporal variations in EROI

Figure 3 illustrate the seasonal spatial distribution of $EROI_A$ and $EROI_B$ for these two scenarios. These show that $EROI_A$ and $EROI_B$ are consistently high in a central-latitudinal band of the African continent (i.e. the Sahel) during both winter ($\approx$2–2.5 for $EROI_A$, $EROI_B$ respectively) and summer ($\approx$3–3.5 for $EROI_A$, $EROI_B$ respectively), whereas North Africa exhibits the expected high seasonal EROI-variation, with some of the highest and lowest values across the irrigated region for the summer and winter respectively. The continental boundaries of the equatorward irrigated region also exhibit high EROI as will be discussed below. Note that this area is presently a grassland/forest transition region (shown in Fig. 1 of Zeng et al., 2008).

The greatest winter increases in NPP (Fig. 4g) are located on the western and central portions of the irrigated region. This portion is mainly driven by increased convergence of northeasterly trade winds and increased monsoonal winds – driven by significantly lower temperatures at the irrigated region mid-latitudes along the coast at this latitude. The wintertime confluence of low insolation (and so NPP) and the relatively low change in continental precipitation, particularly over the irrigated region (Fig. 4e), explains why EROI peaks at a lower irrigation rate during winter. Outside of the irrigated region, wintertime trades advect irrigation water southwest into the Gulf of Guinea and the subequatorial African landmass, corresponding to a decrease in primary production over the irrigated region (Fig. 4g). The greatest summer increases in NPP (Fig. 4h) are along the continental maritime boundary areas, particularly those in the west and north, which border the Mediterranean and the Atlantic Ocean.

3.3 Climatic differences

Such a large scale-modification of the terrestrial surface goes further than the addition of vegetation and localised effects of albedo and surface energy fluxes on climate variables. The extent of desert greening simulated entails highly visible global consequences resulting from the massive increase in moisture input, evaporation (Fig. 4a

ESDD
4, 717–742, 2013

and b) and precipitation (Fig. 4e and f) which culminate in shifts of magnitude, space and time in both regional and global climatology. Note the southward shift in the global Hadley cell (Fig. 4e and f), in agreement with previous studies by Brovkin et al. (1998), Claussen et al. (1999) and Ornstein et al. (2009). A detailed discussion of the mechanics underlying this modelled shift can be found in the paper by Ornstein et al. (2009).

Accompanying this is a marked decrease in NPP and precipitation in South Asia, as the inter-tropical convergence zone (ITCZ) shift alters the positioning of the Indian Monsoon during Northern Hemisphere winter. The impact of increased soil moisture in north Africa on precipitation in the northern portion of South America was studied by Hagos et al. (2005), and is essentially reproduced here (Fig. 4f), evidenced by an increase in both NPP and precipitation in the region. There is also a strong increase in summertime NPP and precipitation in the Mediterranean portion of southern Europe. The latter two impacts are potentially important given the expected increase in frequency and intensity of these regions' respective drought periods under various climate change scenarios (Fussel, 2009).

4 Discussion

This section describes the physical mechanisms underlying our results, based on their agreement with previous studies. Although this is not the central purpose of this paper, the accordance of our findings with other research thereby supports the EROI results. The discussion will first focus on how we can interpret the results to view highest EROI regions from our simulations, and then comment on the physical causes of these locations. The larger scale impacts of desert greening on energy, circulation and precipitation regimes are then treated, followed by a short summary and discussion of the limitations inherent in, and future research implied by, our study.

ESDD
4, 717–742, 2013

4.1 Interpretation of the results

Given the simulation setup, it is not possible to identify the highest EROI, and thereby the most sustainable location(s) for desert greening. The value of the whole-region irrigation scenario undertaken is that it allows us to first identify those areas of highest efficiency within the arid region. The next step would be to filter out these regions where high NPP is a result of a precipitation feedback originating in moisture advection from another area. This would require numerous additional model sensitivities that were not performed here. However, broad-based inferences can be made by examining a suite of basic variables on different spatial and temporal scales, and subjecting these to thermodynamic rules and climatic knowns from previous studies. These we examine below.

4.2 Regions of highest EROI

Regions with the highest EROI occur at the western coastal boundary of Africa. From the maps, we can infer that this occurs due to much higher NPP and precipitation in these areas, which are in turn the result of higher seasonal solar radiation input, and simultaneous greater latent cooling of the landmass during summer compared to winter. The east and northeastern regions see a small precipitation increase during the summer, presumably because the trades and the African Eastern Jet are in operation, as described by Hagos et al. (2005), which comes over the Arabian Peninsula and pulling in hot, dry air from that region, subsequently advects the evaporated irrigation moisture from the northeast to the south, where it is pumped out over the continental African inter-tropical convergence zone (ITCZ), shown in Fig. 4f.

The cluster of grid-cells within the irrigated region in which NPP and precipitation are consistently higher than others during winter and summer is in the southwestern coastal portion of the irrigated region (roughly 12° N, 10° W), owing to its coastal-Equatorial positioning. This implies high year-round solar radiation input, and thus the energy to maintain a monsoon effect year-round.

ESDD
4, 717–742, 2013

These observations have important implications for the EROI analysis of irrigation: maximum sustainability of irrigation requires a maximum precipitation feedback, because if water is evaporated and advected elsewhere, particularly over the ocean, it can arguably be considered "lost" in energy-investment terms. This loss is clearly evident in winter, when most of the change (increase) in precipitation occurs over the Equatorial Atlantic (Fig. 4e), resulting in a systematically lower EROI across the majority of the irrigated region. Overall, from the perspective of EROI-efficiency of irrigation, preferable Desert Greening areas in our simulations are likely to be those on the western and north-western coastal boundaries of our irrigated region in the Sahara/Sahel.

4.3 Interpreting large-scale impacts

The impact of evapotranspiration at both regional and global levels is greatest in the Northern Hemisphere summer, which is consistent with previous studies simulating enhanced African soil moisture (Cook et al., 2004; Hagos et al., 2005; Ornstein et al., 2009). These describe a shutdown of the African Easterly Jet (Hagos et al., 2005; Ornstein et al., 2009), which in the control circumstances retards the monsoonal Westerlies from developing polewards of 15° N. With desert greening, latent cooling due to evaporation and evapotranspiration gives rise to the subsequent domination of monsoonal feedback on circulation and precipitation regimes over the coastal region. This would counteract the surface trades, leading to an increase in coastal SSTs during summer, as can be seen in Fig. 4d, which could degrade coastal-boundary Ekman pumping there, in agreement with previous findings by Ornstein et al. (2009).

These effects are an amplification of circulation patterns already in place in the control or present-day scenario, whereby southerly and northerly winds in conjunction with supply of moisture to the lower troposphere shifts the focal point of convergence from the African coast to the continental interior (Hagos et al., 2007). This change is reflected as a latitudinal shift in maximal precipitation from the Gulf of Guinea in early May to the north of Africa (Hagos et al., 2007). That this effect is amplified in our simulations is supported by the strong decrease in summertime precipitation in the Gulf,

ESDD
4, 717–742, 2013

implying a northward shift of the entire mechanism, driven by the apparent latent heating and enhanced moisture supply to the lower troposphere.

The monsoonal effect appears to drive in the opposite direction in winter: tropical easterly flow over the irrigated region will tend to increase substantially in winter, resulting in high levels of moisture convergence over the Equatorial Atlantic, as was shown by Hagos et al. (2005), and the large increase in winter maritime precipitation seen in Fig. 4c.

4.4 Summary and implications

There are four overarching results from these sensitivity simulations. First, the energy return in many parts of the irrigated region is greater than 1 : 1. This means, perhaps surprisingly, that in conventional investment terms we have excess direct ($EROI_A$) energetic profits averaged over the entire irrigated region of 30 % in winter and 80 % in summer (Fig. 1a). $EROI_B$, which includes the precipitation feedback, increases this to 60 % in winter and to 160 % in summer, an effective doubling. These figures appear to imply that desert greening could be "worth it" in the thermodynamic sense, notwithstanding the energetic cost of outlay and maintenance. Nonetheless, such energetic returns are relatively low compared to those, e.g. of other renewable energy technologies (Hall et al., 1986; Murphy and Hall, 2010).

Second, there are regions of the Western coastal Sahara/Sahel in which the EROI given by irrigating the whole irrigated region can be expected to approximate the EROI of those regions or grid cells if they were irrigated in isolation or small clusters. Although only an indirect and imprecise deduction, the assumption seems reasonable given that we can infer this precipitation to be a direct thermal effect of irrigation quantity, not irrigation scale (at least at this grid-resolution), and that the precipitation is not sourced from irrigation water pumped into other grid cells (see Sects. 4.1 and 4.2).

Third, irrigation of the entire region produces large-scale regional and global teleconnection effects (as also found by Hagos et al., 2005 and discussed in Ornstein et

ESDD
4, 717–742, 2013

al., 2009) proportional to the quantity of irrigation water supplied. This raises concerns of irrigation scale, and would need to be evaluated in more detail in the future.

Fourth, our simulation output is consistent with the findings of other studies which used different climate models and simulation scenarios to estimate the outcome of Desert Greening. Atmospheric circulation changes, teleconnections on both a regional and global scale, shifts of the ITCZ, orographic effects, and even the optimal mean irrigation rate, are supported by previously published research. This gives both the direct output and the inferences made herein a high level of corroboration.

Our $EROI_B$ term extends the definition given by Murphy and Hall (2010) to include the precipitation feedback as an energetic gain. Indeed, since the exergy content of the initial and maintenance capital investment in this Desert Greening scenario have been negated here for simplicity, our $EROI_B$ is equivalent to exergy return on exergy invested, as given in Bakshi et al. (2011).

4.5 Limitations and future research

Considerable research is still needed to grasp the full exergetic content of the carbon farming lifecycle, by expanding the implicit boundaries of the "closed system" used here. Here, we focused our attention on the irrigated region of the Sahara/Sahel, yet these global model simulations also show changes to NPP and precipitation in distant regions of India, the Amazon, Southern Europe, East Asia, and North America. We expect that these changes are in part related to the extreme spatial scale and irrigation intensity of our experimental setup, with these changes being less pronounced if irrigation was only applied to a few dispersed locations. Developing Desert Greening in select locations, such as the southwest coastal region of the Sahara, seem the most promising from the EROI perspective.

Taking these thoughts a bit further, even low-elevation coastal regions will require a large energy source for desalination and pumping. EROI ratios greater than 1 : 1 would enable the harvested plant material to be used as the desalination energy source (e.g. Becker et al., 2012) and still be self-sustaining, with the remainder equivalent to an

ESDD
4, 717–742, 2013

operational profit. This energetic profit may increase further if photovoltaics or concentrated solar power is used as the energy source, especially if these solar technologies were deployed in adjacent locations with a low EROI.

Even with a sufficient energy source for desalination and pumping, desalinated water still contains salts (Elimelech and Phillip, 2011) which would challenge a long-term Desert Greening type strategy for food production or carbon farming. Mitigating strategies such as the full or cyclical use of halophytes as a form of bioremediation (Flowers et al., 2010) and the growth response of arid plants to subsurface drip irrigation (as dust may then accumulate on the leaves) requires further study. This type of plant-type selection is also specific to the intention, as the plant types that maximize food production or maximize water and energy efficiency in the biome might be quite different.

Studies such as Baudena et al. (2008) have shown that "tipping point" regimes between hot/dry and cool/wet states differ substantially between natural and cultivated monoculture vegetation, in which cultivated areas necessitate higher vegetation fraction and initial soil moisture levels in order to sustain the cool/wet state. Other related microscale soil–vegetation–atmosphere feedbacks that induce greater water retention, precipitation, and moisture-recycling over the irrigated area, as discussed with respect to vegetation cover type by Scheffer et al. (2005) and with respect to arid regions in Janssen et al. (2008) require specific investigation, as neither mechanism is included in our model. As Desert Greening can be viewed as a type of agricultural cultivation, utilizing such non-conventional cultivation regimes like agro-ecology and conservation agriculture could be advantageous, possibly even with a focus on perennials (i.e. Jackson, 2011) These types of plant strategies and associated ecosystem responses may have non-trivial implications for irrigation, EROI, and the precipitation feedback and therefore deserve further research.

A related discussion related to desert greening concerns its possibility as a self-sustaining vegetated system, representing one of two alternative stable-states of the Sahara/Sahel (Brovkin et al., 1998; Claussen et al., 1999). This could summarized as: given the necessary areal extent and rate of additional water availability, the precip-

ESDD
4, 717–742, 2013

itation (Charney) feedback which is induced by irrigation and subsequent evapotranspiration sustains a vegetated state of the region (Charney et al., 1975; Ornstein et al., 2009; Becker et al., 2012). Induced by human action rather than changes in the natural environment, this may be possible by temporarily irrigating the region with desalinated water. Should this alternate steady-state result, this would greatly increase the EROI over those simulated in this analysis. Conversely, if such a steady-state exists, it is likely that this "tipping point" scale and water input rate may not coincide with the EROI-optimal locations and irrigation input levels identified herein. As concluded by Becker et al. (2012), we would also expect that at least some human-provided water input would always be required to sustain desert greening in this region, especially in those regions distant from the coast, although the scale of irrigation most likely plays a central role in the extent to which this expectation applies.

Viewed specifically from the EROI perspective, as the net carbon sequestration rate and energy input for desalination and pumping is known, it would be possible to estimate an $EROI_c$ value. To review, $EROI_a$ considers the stored energy content of the plant biomass and the energy input required for desalination and pumping, while $EROI_b$ extends this by additionally including the precipitation feedback. $EROI_c$ would more fully encompass the system dynamics, as there are accompanying changes in albedo due to changes in net global cloud cover and vegetation, thereby causing a change in global radiative forcing induced by irrigating the Sahara/Sahel. Using the approach of Lenton and Vaughan (2009), these differences could be classed into shortwave (albedo) and longwave (atmospheric CO_2) radiative forcing reductions. These reductions could then be multiplied by some representative energetic value for radiative forcing. In this way, $EROI_c$ would consider not only the energetic inputs and outputs required for a given activity such as Desert Greening, but would also include the per energy-unit net radiative forcing reduction. This reduction could then be added to the energy output term (the numerator in Eq. 3).

This type of analysis shows the potential for opening up the scope of EROI to investigate the overall effects of human activities or technological processes – via their

ESDD
4, 717–742, 2013

relative energy inputs and outputs – on the environment at local, regional and planetary scales. For example, the cultivation of certain types of staple crops around the world will have different energy input and (calorific) output ratios, while differently affecting land–atmosphere interactions and gaseous emissions, with attendant impacts on the global energy balance (imagine, for example, rice vs. wheat). Both existing and proposed changes to the makeup of global crops could be subjected to an EROI analysis such as the one undertaken here. Likewise, the composition of, and distribution between, the suite of renewable energy technologies at regional or global scales could also be assessed for relative sustainability using EROI analysis.

5 Conclusions

This study has shown how applying Energy-Return-on-Investment (EROI) to desert greening in the Sahara/Sahel can add a new perspective to such a large-scale human alteration of the Earth system. We find that by quantifying the energy inputs of desalination and pumping, along with the energy output of biomass production, desert greening of this region may be energetically sustainable. This sustainability, as defined by a EROI ratio greater than 1 : 1, has both a spatial and seasonal component. Overall, in response to irrigating the *entire* Sahara/Sahel region at the same rate, the Western Sahara near the coast had the highest EROI of $\approx 6 : 1$ after including the additional precipitation feedback. Recognizing that our experimental setup of irrigating such a large region may be practically problematic due to a variety of logistical and environmental concerns (e.g. changes in global climatology), the outcome that with some irrigation rates, the energy output is greater than the energy input (i.e. EROI $> 1 : 1$) nonetheless implies that desert greening could warrant further investigation. While more research is certainly required before any implementation of desert greening should take place, the benefits in quantifying EROI in a context where human action directly instigates large-scale changes in Earth System dynamics have been demonstrated here.

Acknowledgement. The authors have no competing financial interests.

ESDD
4, 717–742, 2013

References

Bakshi, B. R., Baral, A., and Hau, J. L.: Accounting for resource use by thermodynamics, in: Thermodynamics and the Destruction of Resources, 1st Edn., edited by: Bakshi, B., Gutowski, T. G., and Sekulic, D. P., Cambridge University Press, New York, NY, USA, 87–109, 2011. 720, 723, 731

Baudena, M., D'Andrea, F., and Provenzale, A.: A model for soil-vegetation-atmosphere interactions in water-limited ecosystems, Water Resour. Res., 44, W12429, doi:10.1029/2008WR007172, 2008. 732

Baum, A. W., Patzek, T., Bender, M., Renich, S., and Jackson, W.: The visible, sustainable farm: a comprehensive energy analysis of a midwestern farm, Crit. Rev. Plant Sci., 28, 218–239, 2009. 720

Becker, K., Wulfmeyer, V., Berger, T., Gebel, J., and Münch, W.: Carbon farming in hot, dry coastal areas: an option for climate change mitigation, Earth Syst. Dynam. Discuss., 3, 1221–1258, doi:10.5194/esdd-3-1221-2012, 2012. 722, 723, 724, 731, 733

Brovkin, V., Claussen, M., Petoukhov, V., and Ganopolski, A.: On the stability of the atmosphere vegetation system in the Sahara/Sahel region, J. Geophys. Res.-Atmos., 103, 31613–31624, 1998. 727, 732

Charney, J. G., Stone, P. H., and Quirk, W. J.: Drought in the Sahara: a biogeophysical feedback mechanism, Science, 187, 434–435, 1975. 733

Claussen, M., Kubatzki, C., Brovkin, V., Ganopolski, A., Hoelzmann, P., and Pachur, H. J.: Simulation of an abrupt change in Saharan vegetation in the Mid-Holocene, Geophys. Res. Lett., 26, 2037–2040, 1999. 727, 732

Cook, K. H., Hsieh, J. S., and Hagos, S. M.: The Africa–South America intercontinental teleconnection, J. Climate, 14, 2851–2865, 2004. 729

Elimelech, M. and Phillip, W. A.: The future of seawater desalination: energy, technology, and the environment, Science, 333, 712–717, 2011. 732

Flowers, T. J., Galal, H. K., and Bromham, L.: Evolution of halophytes: multiple origins of salt tolerance in land plants, Funct. Plant Biol., 37, 604–612, 2010. 732

Fussel, H.-M.: An updated assessment of the risks from climate change based on research published since the IPCC Fourth Assessment Report, Climatic Change, 97, 469–482, 2009. 727

ESDD
4, 717–742, 2013

Gebel, J. and Yüce, S.: An Engineer's Guide to Desalination, VGB PowerTech Service GmbH, Essen, Germany, 2008. 723
Gutowski, T. G., Sekulic, D. P., and Bakshi, B. R.: Preliminary thoughts on the application of thermodynamics to the development of sustainability criteria, IEEE International Symposium on Sustainable Systems and Technology, 2009, ISSST'09, Tempe, Arizona, USA, 1–6, 2009. 720
Hagos, S. M., Samson, M., and Cook, K. H.: Influence of surface processes over Africa on the Atlantic marine ITCZ and South American precipitation, J. Climate, 18, 4993–5010, 2005. 727, 728, 729, 730
Hagos, S. M., Samson, M., and Cook, K. H.: Dynamics of the West African monsoon jump, J. Climate, 20, 5264–5284, 2007. 729
Hall, C. A. S., Cleveland, C. J., and Kaufmann, R.: Energy and Resource Quality: The Ecology of the Economic Process, Wiley, New York, 1986. 719, 730
Hansen, J. E.: Scientific reticence and sea level rise, Environ. Res. Lett., 2, 024002, doi:10.1088/1748-9326/2/2/024002, 2007.
Jackson, W.: Consulting the Genius of the Place: An Ecological Approach to a New Agriculture, Counterpoint Press, Berkeley, CA, USA, 2011. 732
Janssen, R. H. H., Meinders, M., Marcel, B. J., Van Egbert, N. E. S. H., and Scheffer, M.: Microscale vegetation-soil feedback boosts hysteresis in a regional vegetation climate system, Global Change Biol., 14, 1104–1112, 2008. 732
Kleidon, A., Fraedrich, K., and Heimann, M.: A green planet vs. a desert world: estimating the maximum effect of vegetation on the land surface climate, Climatic Change, 44, 471–493, 2000. 722
Kubiszewski, I., Cleveland, C., and Endres, P.: Meta-analysis of net energy return for wind power systems, Renew. Energ., 35, 218–225, 2010. 720
Lenton, T. M. and Vaughan, N. E.: The radiative forcing potential of different climate geoengineering options, Atmos. Chem. Phys., 9, 5539–5561, doi:10.5194/acp-9-5539-2009, 2009. 733
Lunkeit, F., Blessing, S., Fraedrich, K., Jansen, H., Kirk, E., Luksch, U., and Sielmann, F.: Planet simulator user's guide version 15.0, Meteorological Institute of the University of Hamburg, Hamburg, 2007. 724

ESDD
4, 717–742, 2013

Miller, L. M., Gans, F., and Kleidon, A.: Estimating maximum global land surface wind power extractability and associated climatic consequences, Earth Syst. Dynam., 2, 1–12, doi:10.5194/esd-2-1-2011, 2011. 720

Murphy, D. J. and Hall, C. A. S.: Year in review EROI or energy return on (energy) invested, Ann. NY Acad. Sci., 1185, 102–118, 2010. 719, 720, 730, 731

Odum, H. T.: Environmental Accounting: EMERGY and Environmental Decision Making, Wiley, New York, NY, USA, 1996. 720

Ornstein, L., Aleinov, I., and Rind, D.: Irrigated afforestation of the Sahara and Australian Outback to end global warming, Climatic Change, 97, 409–437, 2009. 722, 723, 724, 727, 729, 730, 731, 733

Patzek, T. W.: Thermodynamics of agricultural sustainability: the case of US maize agriculture, Crit. Rev. Plant Sci., 27, 272–293, 2008. 720

Peixoto, J. P. and Oort, A. H.: Physics of Climate, American Institute of Physics, New York, USA, 1992. 720

Scheffer, M., Holmgren, M., Brovkin, V., and Claussen, M.: Synergy between small-and large-scale feedbacks of vegetation on the water cycle, Global Change Biol., 11, 1003–1012, 2005. 732

Valero, A. and Valero, A.: A prediction of the exergy loss of the world's mineral reserves in the 21st century, Energy, 36, 1848–1854, 2011. 720

Zeng, X. D., Zeng, X. B., and Barlage, M.: Growing temperate shrubs over arid and semiarid regions in the Community Land Model Dynamic Global Vegetation Model, Global Biogeochem. Cy., 22, GB3003, doi:10.1029/2007GB003014, 2008. 726

ESDD
4, 717–742, 2013

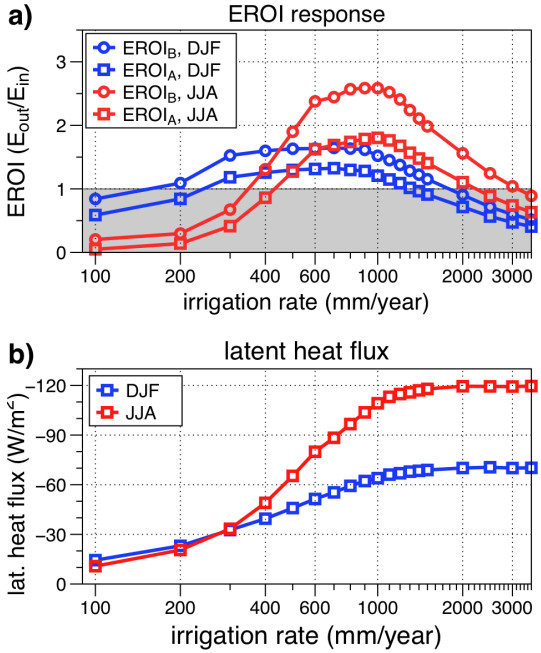

Fig. 1. December to February (blue) and June to August (red) **(a)** EROI$_A$ and EROI$_B$, **(b)** NPP as a function of irrigation rate, averaged over the entire irrigated region.

ESDD
4, 717–742, 2013

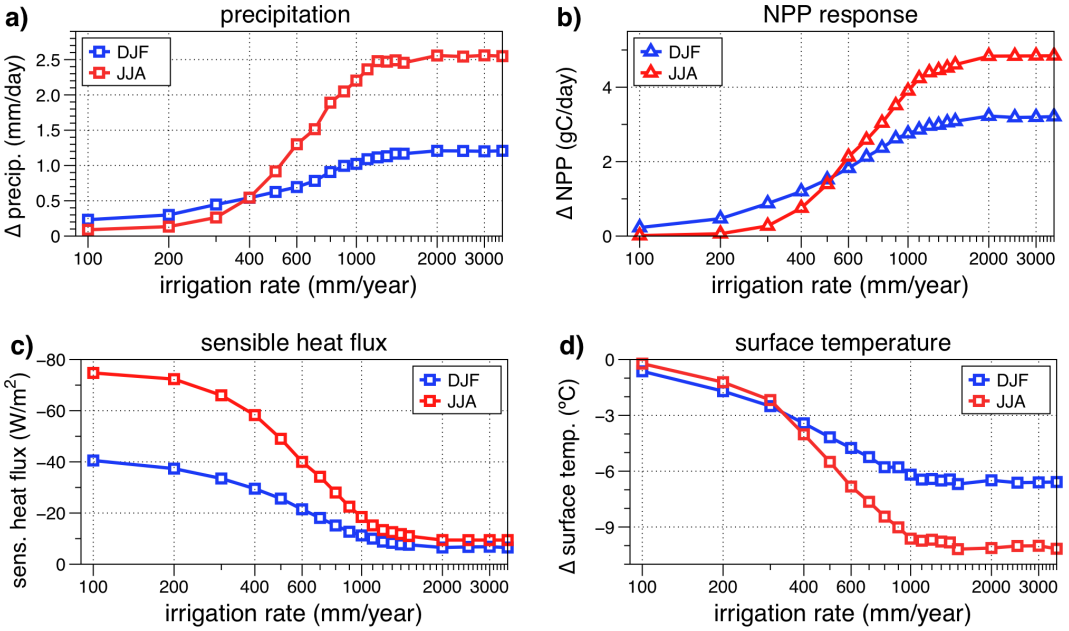

Fig. 2. Seasonal responses of the irrigation rate to common climatological variables: **(a)** precipitation, **(b)** latent heat flux, **(c)** sensible heat flux, and **(d)** surface temperature in response to the increased irrigation rate, averaged over the entire irrigated region.

ESDD
4, 717–742, 2013

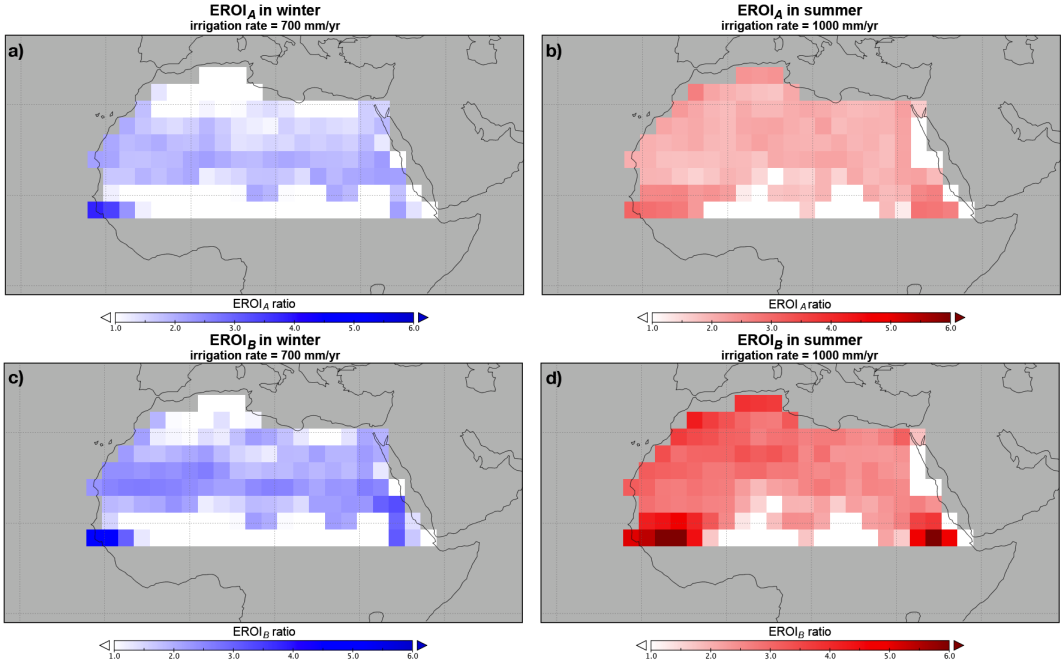

Fig. 3. Seasonal mean EROI$_A$ **(a, b)** and EROI$_B$ **(c, d)** over the irrigated region in DJF **(a, c)** and JJA **(b, d)**. Winter values are taken from the 700 mm yr^{-1} simulations, while summer values are taken from the 1000 mm yr^{-1} simulations.

ESDD
4, 717–742, 2013

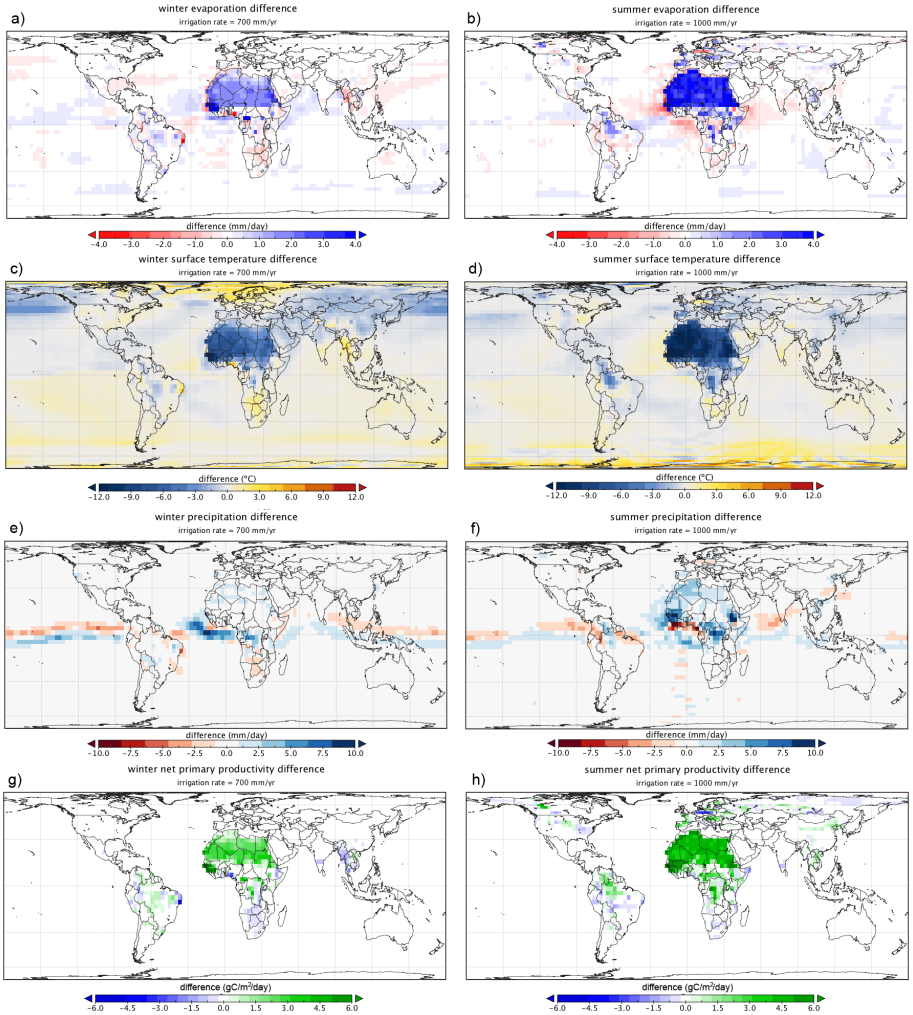

ESDD
4, 717–742, 2013

Energy returns of desert greening

S. P. K. Bowring et al.

Fig. 4. Differences in evaporation **(a, b)**, surface temperature **(c, d)**, precipitation **(e, f)**, and net primary productivity, or NPP **(g, h)** during and winter (left panels) and summer (right panels); *winter* compares the 700 mm yr^{-1} and control simulations for December–February, while *summer* compares the 1000 mm yr^{-1} and control simulations for June–August. Note the significant differences in both variables in regions outside the irrigated region, particularly in southern Africa, southern Europe and northern Latin America. The corresponding southward shift in the inter-tropical convergence zone (ITCZ) is clearly visible in both winter (**e**) and summer (**f**).

ESDD
4, 717–742, 2013